**CONVECTIVE VORTEX AND DUST DEVIL PREDICTIONS IN GALE CRATER, MARS USING A THERMODYNAMIC THEORY AND COMPARISON WITH OBSERVATIONS.** Claire E. Newman[1], Mark I. Richardson[1], Mark Lemmon[2] and Henrik Kahanpää[3], [1]Aeolis Research, 600 N. Rosemead Blvd., Pasadena, CA 91107, USA, claire@aeolisresearch.com, [2]Space Science Institute, 4750 Walnut St, Suite 205, Boulder, CO 80301, [3]Finnish Meteorological Institute, Helsinki, Finland.

**Introduction:** Renno et al. [1], henceforth R98, proposed a thermodynamic theory for convective vortices and dust devils (dust-filled vortices), in which the 'dust devil activity' (DDA) is proportional to the surface sensible heat flux (the energy available to drive vortices) and the vertical thermodynamic efficiency (the efficiency with which this energy is harnessed). The former is proportional to the surface-to-air temperature difference, air density, and drag velocity, while the latter increases with the thickness of the planetary boundary layer (PBL).

This theory allows the DDA - i.e., the expected intensity of vortex activity at any given time - to be predicted from large-scale atmospheric properties, which in turn allows the DDA to be predicted by mesoscale atmospheric models. We show that DDA predictions based on output from the MarsWRF model provide a good representation of the diurnal, seasonal, and spatial variation of vortex activity in Gale Crater, Mars.

**The Renno et al. Theory of Dust Devil Activity:** In R98 the DDA is defined as:

$$\Lambda \approx \eta F_s$$

where $F_s$ is the surface sensible heat flux (the heat input to the base of the vortex) and $\eta$ is the vertical thermodynamic efficiency of the dust devil convective heat engine (the fraction of the input heat turned into work). After some manipulation, $\eta$ is given as:

$$\eta \approx 1 - b \quad , \quad \text{where:}$$

$$b \equiv \frac{(p_s^{\chi+1} - p_{top}^{\chi+1})}{(p_s - p_{top})(\chi+1)p_s^{\chi}}$$

and where $p_s$ is the ambient surface pressure, $p_{top}$ is the ambient pressure at the top of the convective boundary layer, and $\chi \equiv R'/c_p = 0.25$ for Mars. In MarsWRF, the sensible heat flux is given by:

$$F_s = C_d \rho u^* (T_{surf} - T_{air})$$

where $C_d$ is a drag coefficient that depends on the stability of the near-surface atmosphere, $\rho$ is air density, $u^*$ is drag velocity, and $T_{surf}$ and $T_{air}$ are the surface and lowest layer air temperatures, respectively.

**The MarsWRF Multi-Scale Model:** MarsWRF is run as a 2° resolution global circulation model with five nested domains centered over the NW quadrant of Gale Crater. Each domain covers a smaller area than its parent at three times the horizontal resolution, resulting in a resolution of ~450m in the innermost nest (domain 6). Meteorological variables $P_s$, $P_{top}$ , $F_s$, $\rho$, $u^*$, $T_{surf}$ and $T_{air}$ are output from domains 5 (covering all of Gale Crater) and 6 every Mars minute, allowing the DDA and its contributing factors to be computed.

**Vortex Pressure Drops Seen by Mars Science Laboratory (MSL):** When part of a convective vortex passes over the rover its signature is seen as a rapid, shortlived pressure drop due to the vortex's low pressure core, in addition to often producing rapid simultaneous fluctuations in wind direction and air temperature, and (more rarely) a decrease in UV flux if the vortex is sufficiently dusty [2]. We focus on pressure drops and use a method similar to that described by [3]: move through the Rover Environmental Monitoring Station (REMS) pressure dataset in 60s sliding windows, perform a linear fit to pressure in the first and last 15s, then look at the difference between the linear fit and actual pressure at the center of the period. As in [3] and [4] we look for drops exceeding 0.5 Pa.

**MarsWRF Predictions:** Fig. 1 shows MarsWRF predictions of DDA, sensible heat flux and thermodynamic efficiency at 3 times of day around local summer solstice (Ls~270°), a time of peak solar forcing.

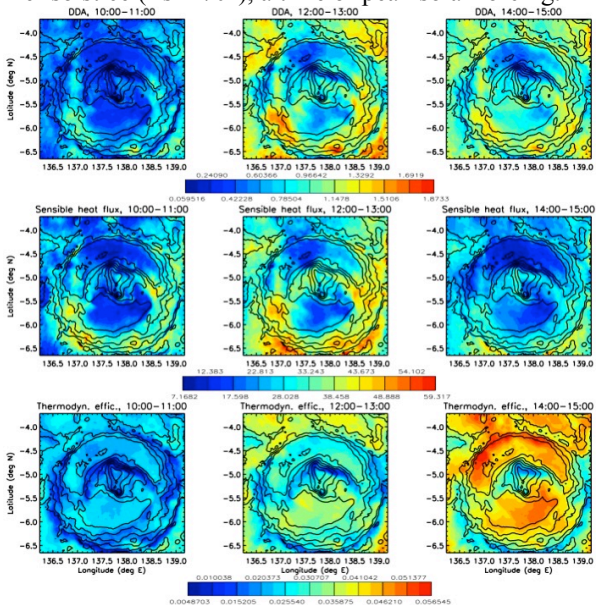


*Figure 1: DDA (top), sensible heat flux (middle) and thermodynamic efficiency (bottom row) at southern summer solstice (Ls~270°) in three daytime periods: 10:00-11:00 (left), 12:00-13:00 (middle), and 14:00-15:00 (right column) LTST. Black contours show topography (contour interval 500m).*

It is clear that the pattern of DDA has strong similarities to the pattern of sensible heat flux. Interestingly, in many areas the latter acts in the opposite direction to thermodynamic efficiency. For example, while thermodynamic efficiency inside the crater peaks in the trench and is lowest over Aeolis Mons, the sensible heat flux has a peak over most of Aeolis Mons and is low over much of the trench, especially the regions with low DDA. However, the DDA minimum that stretches east across the northern slopes of Aeolis Mons is directly linked to the strong minimum in thermodynamic efficiency there.

It has been suggested that the PBL thickness (hence thermodynamic efficiency) may be larger over Aeolis Mons than in the crater trench, but in the model this is not the case in southern summer, when vortex activity peaks. In this season, there is a thicker PBL in the trench, although in *other* seasons (not shown) - including the landing season, at which many studies were performed - it is indeed thicker over Aeolis Mons.

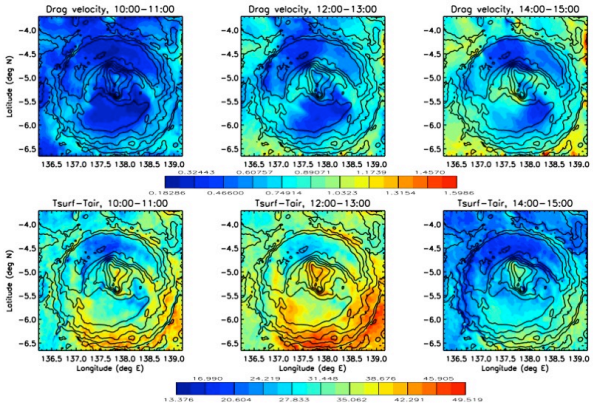


*Figure 2: As in Fig. 1 but now showing u* (top row) and surface-to-air temperature difference (bottom row).*

Fig. 2 shows the main contributors to spatial variation in sensible heat flux: $u^*$ and $T_{surf}$-$T_{air}$. The latter's pattern is due primarily to the spatial variation of surface properties inside the crater. In particular, it is almost the inverse of the thermal inertia map used by MarsWRF in the domain 5 nest, shown in Fig. 3.

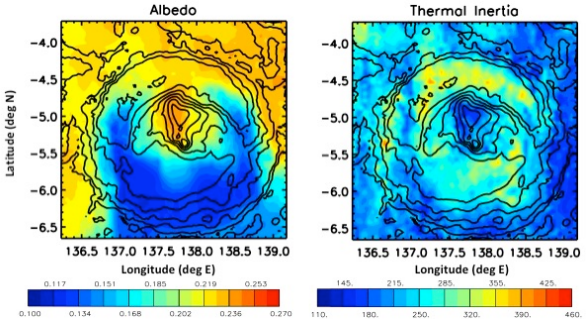


*Figure 3: Albedo (left) and thermal inertia (right) maps used in domain 5 of the MarsWRF simulation.*

This is due to lower thermal inertia causing the surface to warm more rapidly after sunrise, resulting in a larger surface-to-air temperature difference over most of the day. The correlation is weakened over Aeolis Mons and strengthened in a N-S strip at ~137°E, however, due to albedo being higher over Aeolis Mons and low over the strip, but this is a secondary effect.

Fig. 4 shows a comparison between the MarsWRF-predicted DDA and the number and size of observed REMS pressure drops, as a function of time of day, season, and mission year. DDA match the observed peak in vortex pressure drops around noon local time in most seasons, the observed peak in local summer and minimum in local winter, and also the year-to-year increase in vortex pressure drops in most seasons as MSL climbed Aeolis Mons. According to the model, this results from the decrease in thermal inertia (hence surface-to-air temperature difference) and increase in wind speed along MSL's traverse up the slope, both of which result in larger sensible heat fluxes to drive convective vortex activity.

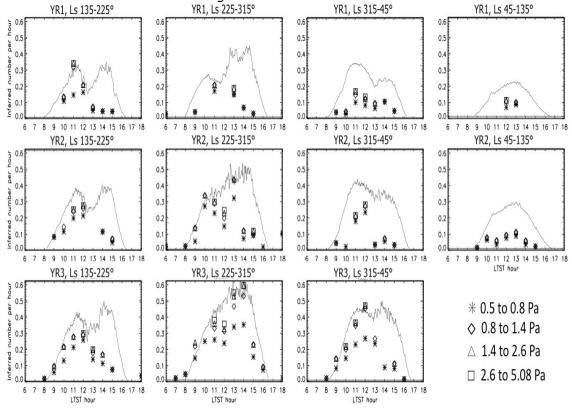


*Figure 4: MarsWRF-predicted DDA (lines) and REMS pressure drops (symbols) as a function of time of sol, over seasonal periods centered around local spring (column 1), summer (column 2), fall (column 3) and winter (column 4), in years 1 (top), 2 (middle) and 3 (bottom row) of the mission.*

**Summary:** The predicted pattern of sensible heat flux is controlled largely by surface thermal properties and the interaction of crater slope winds with larger scale circulations, resulting in a pattern that is somewhat anti-correlated with the thermal inertia map used in the simulation and has a peak on the western, eastern and upper slopes of Aeolis Mons. MarsWRF results suggest the variation in sensible heat flux must be considered when explaining observed spatial and temporal variations in vortex and dust devil activity.

[1] Renno N. O. et al. (1998) *JAS*, *55*, 3244–3252. [2] Kahanpää H. et al. (2016) *JGR*, *121*, 1514–1549. [3] Ordonez-Exteberria I. et al. (2018) *Icarus*, *299*, 309-330. [4] Steakley K. and Murphy J. (2016) *Icarus*, *278*, 180–193.